ELSEVIER

Journal of Alloys and Compounds 253–254 (1997) 185–190

Journal of ALLOYS AND COMPOUNDS

Material characteristics and behaviour of highly deuterium loaded palladium by electrolysis

Naoto Asami[a,*], Toshio Senjuh[a], Hiroshi Kamimura[a], Masao Sumi[a], Elliot Kennel[a], Takeshi Sakai[b], Kenya Mori[c], Hisashi Watanabe[d], Kazuaki Matsui[a]

[a]*R and D Centre for New Hydrogen Energy, The Institute of Applied Energy 3-5, Techno Park 2, Shimonopporo, Atsubetsu-Ku, Sapporo, Hokkaido 004, Japan*

[b]*Nuclear Fuel Industries Ltd., Sapporo, Hokkaido 004, Japan*

[c]*Tanaka Kikinzoliu Kougyou Ltd., Sapporo, Hokkaido 004, Japan*

[d]*NEDO, Sapporo, Hokkaido 004, Japan*

Abstract

Studies on several kinds of palladium cathodes have been conducted in electrochemical cells using $LiOD/D_2O$ electrolyte to determine necessary and sufficient conditions for attaining high deuterium loading. Comparative observations of the microstructure and analysis of surface impurities have been carried out on palladium specimens with various pre-electrolysis treatments and post electrolysis. From the observations and analysis of various processed and treated Pd specimens, the material characteristics of a Pd cathode achieving high loading ratios ($D/Pd>0.85$) are discussed.

Keywords: Palladium; Deuterium; Loading ratio; Microstructure

1. Introduction

A research and development project, referred to as the ''New Hydrogen Energy'' project [1], was started in Japan in November 1993, with the main goal of reproducing and verifying the existence of excess heat generation. during electrolysis in Pd-LiOD systems. It has been supposed that the reproducibility of these phenomena is mainly dependent upon achieving control of cathode material properties as well as the electrolysis environment. It has been pointed out by several observers that attaining a deuterium loading ratio (that is, the ratio of deuterium to palladium atoms) greater than 0.85 is a prerequisite for observing excess heat generation phenomena [2,3]. Thus, achieving high reproducibility of anomalous effects depends upon achieving reproducible high deuterium loading ratios. Material development has proceeded according to this concept.

2. Experimental procedure

2.1. Electrolysis cell and system

Deuterium loading experiments were carried out to verify the excess heat generation during the electrolysis of heavy water with Pd electrode using fuel cell type electrolysis cells [4]. A schematic diagram of the electrolysis cell is shown in Fig. 1. The inner wall of the cell body containing 1 M $LiOD/D_2O$ electrolyte was coated with a silicon-based ceramic film. The Pd cathode, fuel cell anode, reversible hydrogen electrode and thermocouple were fixed in the cell body. Electrolysis was performed with a constant direct current and the current value was changed after equilibrium conditions had been well established for a given temperature of the electrode, electrolyte and gas phase, and deuterium over-voltage at the cathode. The deuterium loading ratio, D/Pd, is determined by calculation from the D_2 gas pressure drop in the closed cell.

*Corresponding author.

0925-8388/97/$17.00
PII S0925-8388(96)03069-1

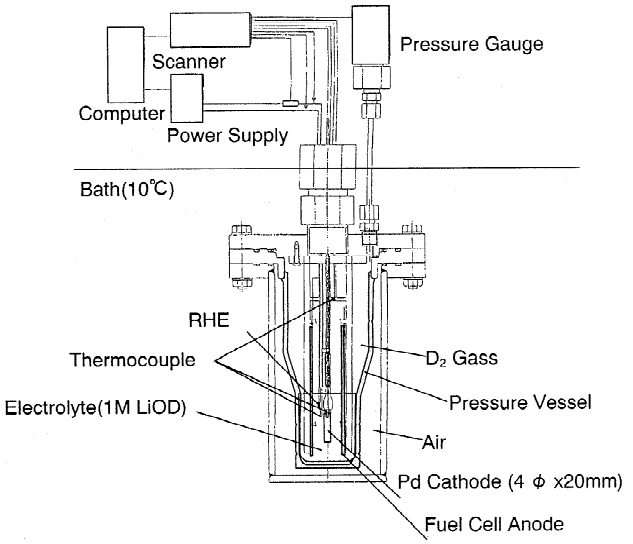

Fig. 1. Schematic diagram of the electrolysis cell.

2.2. Material preparation

Various Pd cathode materials were prepared and examined to determine their suitability for achieving high deuterium loading. The Pd materials and electrolyte used in the series of experiments are tabulated in Table 1. A Commercially available rod (TK-A) was cast in a radio frequency induction-heated furnace in air with an oxidation resistant material. It was then worked by a swaging machine at ambient temperature. A single crystal (TK-AS) was prepared using the floating zone melting method in an argon atmosphere using a TK-A rod as the source material. High purity (>99.995) rods (TK-VA) were cast in vacuum and worked at room temperature. The higher defect density surface zone was removed by machining the outer 200 microns. Other high purity (>99.99) rods (JM-Z) were cast in a hydrogen-nitrogen atmosphere, and worked and annealed before final 20% reduction. After the electrodes were machined to final dimensions (4.0 mm×20 mm length), their surfaces were polished using diamond paste or diamond spray, and the surface was cleaned with acetone, ethanol, and purified water in an ultra-sonic cleaner. Several finishing treatments were examined to remove surface impurities and to make a clean activated surface. Both acid etching for ten minutes in concentrated aqua regia and high-temperature vacuum annealing (~850–1000 °C for 10 h in a $<5\times10^{-6}$ vacuum) were used. Heat treatment under high vacuum and high temperature results in both recrystallisation and surface cleaning by thermal etching.

2.3. Observation methods and impurity analysis

Pre-electrolysis and post-electrolysis observations of the microstructure of the specimens were performed using OM, SEM, and FE-SEM, and the impurity analyses were carried out by means of AES, SIMS and EPMA. The measurements of lattice parameter and phase changes were made by X-ray diffraction.

3. Results of deuterium loading

A typical history of current density, D/Pd ratio; input power and excess heat are shown in Fig. 2 for the case of TK-VA-3. At the beginning of electrolysis the current

Table 1
Material list of Pd samples used in experimental series

Lot No.	Purity (major impurities)	Special process	Etching	Heat treatment	Hv: Hardness	Attained loading ratio Max. D/Pd(H/Pd)	Range
TK-A	>99.95 Pt,Ag,Al,B,Ca	Cast in air	–	As cold worked 200 °C evacuate	141	0.83(0.87)	0.80–0.83
TK-AS	>99.97 Pt,Ag,Al,Fe	Single crystallize by floating zone	–	200 °C evacuate	–	0.89	0.87–0.89
TK-VA-1	>99.995 Fe,Sn,Au	Cast in vacuum 0.2 mm removed	–	As cold worked 200 °C evacuate	106	0.82	0.80–0.88
TK-VA-2	ditto	ditto	–	1000 °C×100 h in Vac<$5\cdot10^{-6}$ torr	59	0.90	0.85–0.90
TK-VA-3	ditto	ditto	Aqua-regia.	1000 °C×10 h in Vac.<$5\cdot10^{-6}$ torr	–	0.91(0.94)	0.85–0.91
TK-VA-4	ditto	ditto	–	850 °C×10 h in Vac<$5\cdot10^{-6}$ torr	–	0.88	0.83–0.88
JM-Z-1	>99.99	Cast in H^2-N^2	–	As 20% worked 200 °C evacuate	–	0.85	0.83–0.85
EH-L1-1	>99.8 Ca, Si, Pt, B, Al	Received from SRI	–	850 °C×3 h in Vac.<$5\cdot10^{-6}$ torr	–	–	-
IM-VB-1	>99.95	Cast in air	Aqua-regia	200 °C evacuate	–	0.88	0.87–0.88

Note; Manufacturer=TK: Tanaka Kikinnzoku Kougyou, JM: Johnson Mathey, EH: Engelhart, IM:IMRA Material, Sample size=final size 4 mm ϕ×20 mm, Electrolyte=1 M LiOD/D^2O, Purity of D^2O:>99.9% (<0.1%H_2O) Hv: Vicker's hardness, Etching: 10 min. in aqua-regia at room temp.

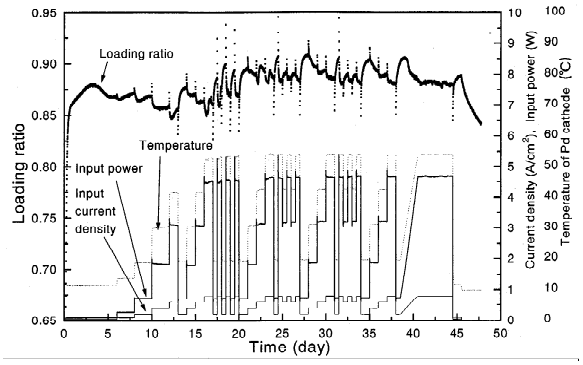

Fig. 2. Typical history of loading ratio D/Pd input current input power and temperature of Pd cathode (TK-VA3).

density was set at 50 mA cm^{-2} for 6 days, and then the current density was changed step by step to 100, 200, 400, and 600 mA cm^{-2} for two days at each level. After this current cycle, the current density was decreased abruptly to 200 mA cm^{-2} and again stepped up to 800 mA cm^{-2}; followed by additional high current pulses or ramps. These changes of electrolysis conditions were performed to investigate the dependence of the D/Pd ratio and excess heat generation upon current density. In this case, the maximum D/Pd reached 0.91 at 200 mA cm^{-2} and 0.89 at 800 mA cm^{-2}, 28 and 24 days after the start of electrolysis respectively. The loading ratios attained by similar electrolysis conditions described as above, are listed in Table 1 for several Pd materials.

4. Results of material observations and analysis

4.1. Microstructural change during loading and deloading

Single-crystal Pd samples (TK-AS) absorbed deuterium slowly. However, the maximum loading ratio reached the rather high value of 0.89. Many regular slip-bands, about 2 μ in breadth, along the (111) plane, were observed on the surface as shown in Fig. 3a–b. The X-ray diffraction pattern of the post-electrolysis specimen shows that the sample no longer has a purely single-crystalline structure. Several internal crack-like defects are observed in the post-electrolysis specimen as shown in Fig. 3c. These might be caused by the deformation of the crystal due to deuterium absorption and transitions between the α and β phases.

The surface structure of high-purity polycrystalline Pd (TK-VA) after high-temperature vacuum annealing is shown in Fig. 4a. Grain boundaries and fine surface structures are observed in the grains as shown in Fig. 4b, which were probably formed by thermal etching in high vacuum. Fig. 4c shows the surface structure of TK-VA-X after electrolysis. Several cracks along the grain boundary are observed and fine slip-band bands are also observed in the crystal grains. The basic mechanism of the formation of slip-bands is presumed to be the same as for the case of single-crystal samples.

The microstructure of EH-L1 specimens before electrolysis and after are shown in Fig. 5a–c. The average grain size is about 200 μ. Sub-grain-like fine structures are observed at the inside of initial grains on the etched surface. Fine granulation seems to be proceeded by the transition between α and β phases.

Fig. 6a–b show the cross-sectional views of a relatively low loaded state. The α+β phase region progresses radially toward the centre and fine granulation is also observed in the initial grains. Diffusion enhancement at grain boundaries, which is normally expected, seems to have less effect in this system.

Fig. 7a–b show that blistering due to deuterium gas occurred on the surface of electrode during electrolysis in some annealed specimens. Clear cracks along the grain boundaries were formed on the top of the blistering. This phenomenon may be explained by assuming the existence of some kind of defects such as closed pore, inclusion, or plane shaped imperfection near the surface before elec-

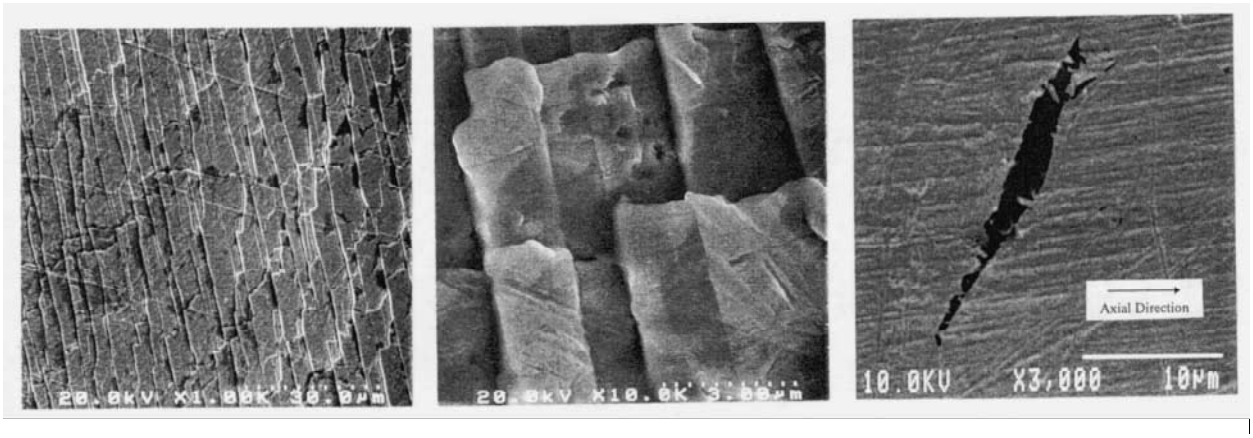

Fig. 3. Regular slip-bands as observed by FE-SEM (a,b) on the surface of post electrolysis single crystal (TK-AS). Internal crack defect in the post electrolysis single crystal (TK-AS) as observed by SEM (c).

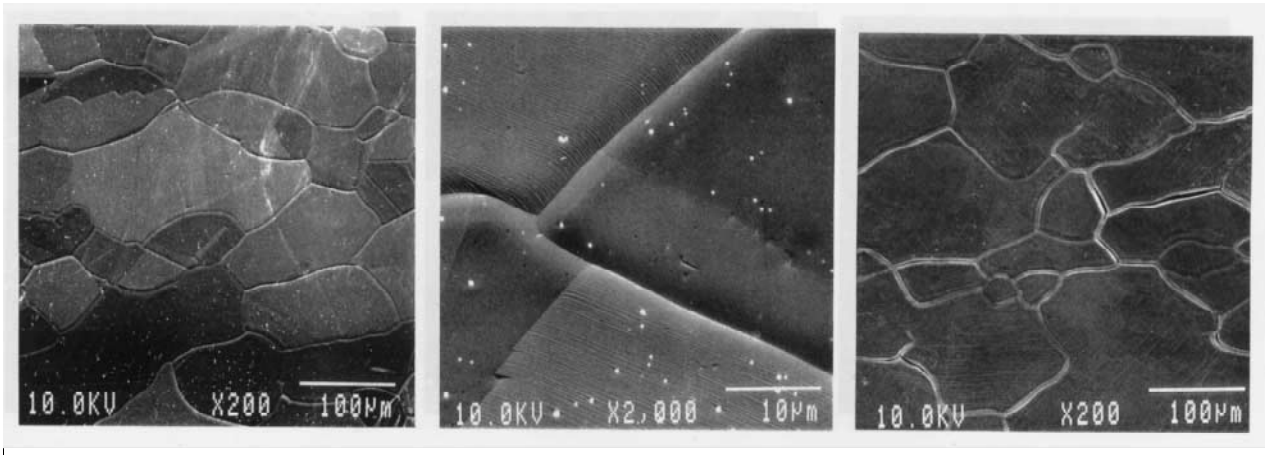

Fig. 4. Surface structure of TK-VA annealed at 1000 °C×10 h in high vacuum ($<5\times10^{-6}$ torr). Grain boundary and fine surface structures in the grain probably formed by thermal ethcing in high vacuum (b). Several cracks along the grain boundary and fine slip bands are observed in the crystal grains of the sample after electrolysis (c).

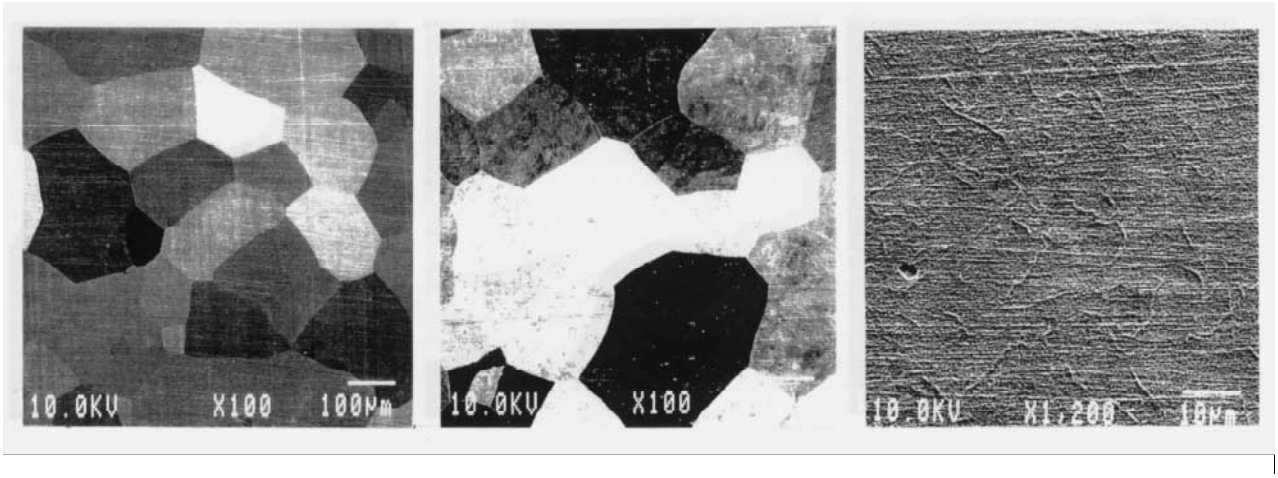

Fig. 5. Polished and etched surface structure of cross section of EH-L1 before (a), and after (b and c) electrolysis. Sub-grain-like fine structures are observed at the inside of initial grains (c).

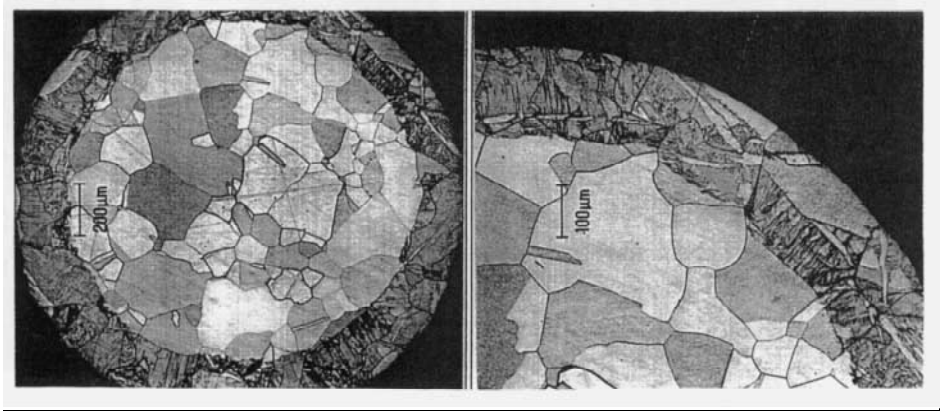

Fig. 6. Cross section view of relatively low loading state of TK-VA. The $\alpha+\beta$ region progresses radially toward centre and fine granulation is advanced.

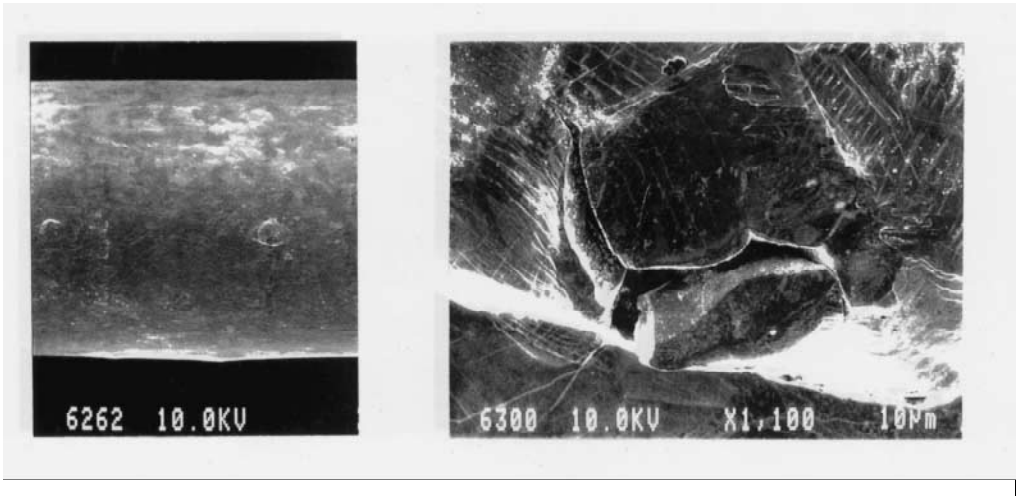

Fig. 7. Blistering due to deuterium gas occurred on the surface of the electrode during electrolysis in some annealed specimens (TK-VA). (b) shows the top structure of blistering and several cracks are formed along the grain boundary.

trolysis. Deuterium gas may accumulate in the defect and, as a result, the gas pressure locally increases several hundred-fold. The annealed surface is then deformed by blistering.

4.2. Surface impurity analysis

Fig. 8a shows the results of AES surface impurity analysis after electrolysis. Impurities such as S, Cl, C, and O are detected in most postelectrolysis specimens. However, it is confirmed by an ion-sputtering method that the impurity layer is less than 2 nm thick. The existence of C and O is confirmed by EPMA analysis. Fig. 8b shows the depth profile of the near-surface region of the palladium cathode by AES. The penetration of Li atoms from LiOD into the Pd cathode was confirmed by SIMS. The penetration depth ranges from several tens to a hundred nm, according to the depth profile analysis.

5. Discussion

Deuterium absorbed into the Pd crystal is expected to occupy the octahedral sites of the fcc Pd lattice for D/Pd ratios up to unity, and tetrahedral sites for ratios above unity. It is believed that the tetrahedral site of Pd acts as a transient site for the diffusion process.

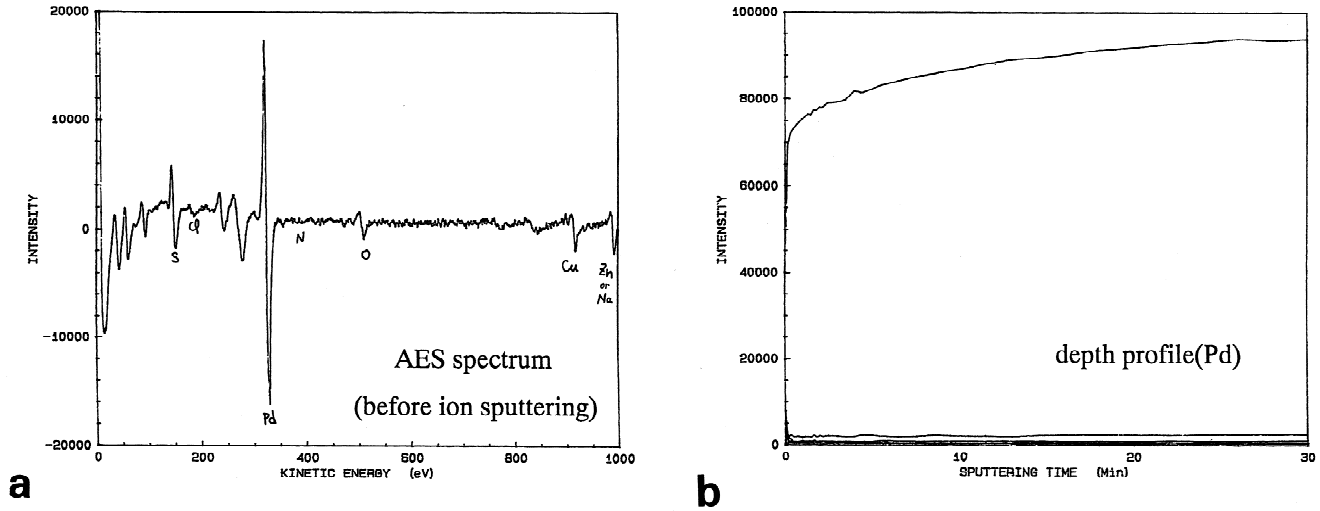

Fig. 8. AES surface impurity analysis after electrolysis (TK-A). Impurities of S, Cl, C, and O are detected in most post electrolysis specimens (a). Depth profile of palladium atoms on the near surface region after electrolysis is shown in (b). The penetration of Li atoms from LiOD into the Pd cathode is confirmed by SIMS analysis.

Table 2
Basic characteristics of high loading material and corresponding treatments

Favourable material state	Corresponding treatments
(1) Make vacant state of absorption site (O-site)	
Remove impurity atoms on O-site	High purity material, vacuum melt, and
Reduce inclusion/precipitates/closed pore	evacuate at high temp., ultrahigh vacuum
(2) Maximize absorption area & not reduce	
Remove surface bad impurities	Ultra-sonic cleaning, etching by aqua-regia
	High vacuum & high temp. treatment
Prevent absorption of bad impurities	Purification of electrolyte
(3) Minimize dissociation area & prevent increment	
Remove surface macroscopic crack	Surface machining, annealing stress
Reduce open pore, surface inclusion	Vacuum melt, clean working processing
Reduce closed pore, defect in near surface	Vacuum melt, homogenized treatment
Reduce surface scratch, roughness	Fine surface polishing
Minimize dissociation channel	Suitable grain size, homogenization
(4) Suppress dissociation quantity during electrolysis	
Keep ductility/toughness against deformation	Suitable grain size, Additional cold working
Keep high loading ratio at high current density	Optimize electrolysis condition,

From the simplified considerations, the basic requirements for a Pd material capable of achieving a high loading ratio are as follows:

1. to have large numbers of vacant absorption sites (O-sites);
2. to have a large absorption area during electrolysis;
3. to minimise dissociation area and prevent the incremental loss of deuterium;
4. to minimise the quantity of dissociated deuterium during the electrolysis process.

Table 2 shows the favourable state, mentioned above, and the corresponding material treatments. From these considerations, the specification of Pd materials and the treatments leading to high loading ratio have been selected as follows:

(A) Specification: (1) Initial purity$>$99.99%, (2) vacuum melt, (3) forging and annealing to homogenise, (4) machining the outer 0.2 mm to remove surface defects.

(B) Treatment: (1) Surface cleaning and etching by aqua-regia to remove surface impurities, (2) Ultrahigh vacuum (oil free) high-temperature annealing to recrystallise and to form an activated surface.

The TK-VA material series of Table 1 is made on the basis of this concept, and achieved the highest loading ratio of 0.91. Further modifications are necessary to prevent blistering, crack formation at grain boundaries, and loading reduction at higher current-density. The material must maintain good ductility and resistance against the deformation due to the release of stress which accompanies deuterium loading and transformation. The effects of deposition of surface impurities and Li penetration have to be clarified.

Acknowledgments

The New Hydrogen Energy Project has been supported under the direction of the New Energy and Industrial Technology Development Organization (NEDO). The authors are indebted to Prof. Okamoto, Prof. Ikegami, Dr. Kunimatsu and all of the NHE-committee members for their guidance and valuable advice in promoting the NHE-Project.

References

[1] N. Asami, K. Matsui, F. Hasegawa, Proceedings of the 5th International Conference on Cold Fusion, April 9–13, (1995) Hotel Loews, Monte-Carlo, Monaco. p. 87
[2] M.C.H. McKubre, et al., Frontiers of cold fusion, in: H. Ikegami (Ed.), Proceedings of the Third International Conference on Cold Fusion, October 21–25, Nagoya, Japan, University Academic Press, Tokyo, 1992, p. 5.
[3] H. Kamimura, T. Senjuh, S. Miyashita, N. Asami, To be presented in ICCF-6, October 13–18, Hotel APEX Toya, Japan. To be published in the Proceedings.
[4] K. Kunimatsu, et al., Frontiers of Cold Fusion, in: H. Ikegami (Ed.), Proceedings of the Third International Conference on Cold Fusion, October 21–25, Nagoya, Japan, University Academic Press, Tokyo, 1992, p. 31.